Technical Design Report

Washington State University-Everett with Everett Community College

MAY 28TH, 2020

Team Members

Austin Carver WSU-Everett Team Lead	Sarah Hastings WSU-Everett Aerodynamics	Kaitlin Jones EvCC Rotor FEA Analysis	Isaiah Funston WSU-Everett Wind Farm Layout
Brian Taylor WSU-Everett Turbine Design	Jackson Wagner WSU-Everett Electrical/Control Design	Sam Ayars EvCC EvCC Lead	Vicky Lam WSU-Everett Financial Planning
Kaleb Willis WSU-Everett Rotor Design	Daniel Richards WSU-Everett Mechanical Design	Zach Paish EvCC Manufacturing	Bob Neary WSU-Everett Mechanical Design

Advisors

Dr. Gordon Taub WSU-Everett Principle Investigator	Joe Graber EvCC Co-PI	Mike Patching EvCC Co-PI	Dr. Jacob Murray WSU-Everett Co-PI

PITCH AERONAUTICS

BRIGHT RAIN SOLUTIONS

Executive Summary

The research presented in the following document was conducted through participation in the Department of Energy's CWC for 2020. The Washington State University Everett Wind Energy team, in collaboration with Everett Community College Wind Energy team, explore the viability of variable pitch vertical axis wind turbines, also known as cycloturbines, as a means of producing reliable power en masse. Vertical axis turbines exhibit a main shaft on an axis that is perpendicular to the wind streamlines and vertical to the ground. A cycloturbine is similar to a traditional fixed pitch turbine but has the ability to adjust the blades dynamically resulting in a significantly greater power output. Fixed pitch systems are known to typically be less efficient than horizontal axis turbines but with the use of a variable pitch system, the efficiency can be notably improved. This subset of turbine design has great potential, they are easier to manufacture and maintain, but has yet to be researched and understood as rigorously as other turbine designs. This research includes, but is not limited to, analysis of wind through cycloturbines, mechanical turbine designs, and the control systems needed to operate the cycloturbine efficiently. Analysis of wind characteristics as it passes through turbines is critical in being able to fully understand and optimize these energy capturing systems. This year's participation included development of blade-element momentum codes to implement flux-line theory, which is a newly developed mathematical model for momentum analysis of wind flowing through cycloturbines.

To meet the objectives of the competition, we chose to implement various design methods. A passive pitch control system is used to ensure higher power coefficients, an active yaw control to adjust for wind direction, and a control system that can limit power and shut down at runaway speeds. When designing cycloturbines, there is a trade-off between the ability to self-start and higher power coefficients at increased speeds. To accommodate this trade-off, we designed a pitch control system that features multiple control schemes which can be changed during operation. Finite element analysis was used to evaluate the strength of the rotor design. The focus for these studies was on centrifugal loads acting on the rotor. The results of this analysis showed weaknesses in the initial designs which were then corrected to meet our desired factor of safety of 2. The various actuators and sensors in the turbine assembly are controlled through an Arduino Uno microcontroller which continuously adjusts the rotor based on the current wind conditions. A power electronics system was designed to convert the 3-phase variable generated voltage into a constant 12 V DC output. An iterative design process has been implemented in the development of the mechanical components. The first prototype was built and tested to failure. The knowledge gained in this process was used to significantly improve the current turbine design.

The team has spent the year strengthening our understanding of wind energy concepts and applying such an understanding to our project development. Choosing to focus our efforts on a cycloturbine design allowed us to participate in active research and immerse ourselves in a growing field. Extensive progress has been made and we look forward to building our prototype and continuing our research.

Table of Contents

I. Introduction

Traditional horizontal axis wind turbines have been researched and developed for decades. They are functional, well understood, proven designs. Vertical axis wind turbines, by contrast, are not as well understood and generally produce less power. Both turbine types have their advantages and disadvantages; horizontal axis wind turbines produce high power and are easily scalable, while vertical axis wind turbines are easier to manufacture and maintain. Our team picked a vertical axis design because vertical axis wind turbines are not as well understood and have a lot of room for research. The goal of this competition is to learn, and we felt we could do that best with a vertical axis wind turbine.

The aerodynamics of horizontal axis wind turbines (HAWTs) are relatively straightforward. There are software packages available, such as QBlade, that can rapidly analyze the aerodynamics of a HAWT. HAWT blades undergo steady forces, that is, each point on a HAWT blade experiences a uniform aerodynamic force regardless of its angular position. Vertical axis wind turbines (VAWTs), have significantly more challenging aerodynamics. VAWT blades are subject to cyclically varying aerodynamic forces. A blade producing useful lift on one side of the turbine may be completely stalled on the other side of the turbine. These cyclically varying forces are largely responsible for the poor performance of traditional VAWTs. Most VAWTs have fixed-pitch blades. Their blades are set at some constant angle with respect to the turbine. When a fixed-pitch VAWT spins, there is nothing to prevent the blades from stalling at some locations, which impairs their performance. Our design is a variable-pitch VAWT, also called a cycloturbine. Cycloturbine blades pitch as the turbine spins to respond to the varying aerodynamic forces, which greatly increases their performance. The blades can be pitched to maximize their performance and prevent stall. **Figure 1** shows an example of the cyclic blade motions of a cycloturbine.

Cycloturbines have been shown to produce much more power than fixed-pitch VAWTs [2], even being competitive with HAWTs, which is why our team chose to design one. Vertical axis wind turbines offer several advantages over traditional horizontal axis wind turbines (HAWTs). HAWTs have their machinery high up in a nacelle, which is difficult and hazardous to maintain, while VAWTs have all their machinery easily accessible on the ground. HAWTs have varying wind velocities along their blades, so their blades are twisted and tapered to account for this, which improves their efficiency, but makes them difficult to manufacture. VAWT blades, by contrast, can have constant profiles which make them easier to construct. Additionally, VAWTs have their center of gravity closer to the ground, making them more suitable for offshore applications than HAWTs, which are difficult to keep upright when offshore.

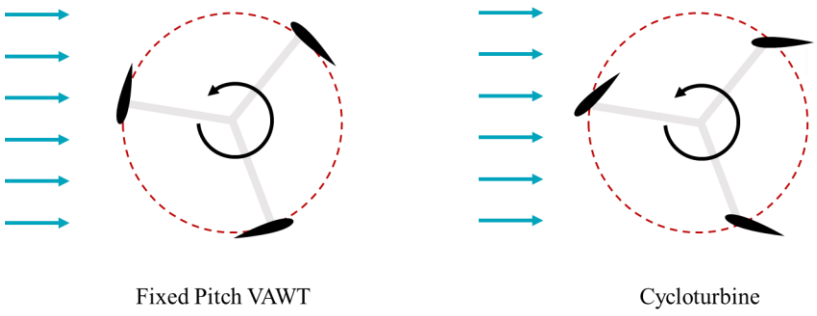

Figure 1: *Fixed Pitch VAWT vs Cycloturbine*

However, cycloturbines are difficult to analyze and have a more complicated mechanical design than either HAWTs or fixed-pitch VAWTs. In this paper we will discuss the design of our cycloturbine, which was designed to compete in the 2020 Collegiate Wind Competition (CWC). An overview of our design and design decisions can be found in **Section II**. The details of our aerodynamic analysis can be found in **Section III**, while the rest of our mechanical design can be found in **Section IV**. Our electrical and control system design are described in **Section V**. The experimental verification of our prototype (planned or otherwise), is in **Section VI**, and our conclusion is in **Section VII**.

II. Design Objectives and Components

The primary design objective for the team was to develop a functional variable pitch vertical axis wind turbine, also called a cycloturbine, to compete in the Department of Energy's CWC. In order to be eligible for the competition as a CWC class turbine, several design requirements needed to be met. The wind energy capturing rotor must fit in the designated 45 cm cubic volume and the rest of the components and structure of the system must occupy a 15 cm cylindrical column extending downward to the mounting table. The column has a maximum length of 60 cm measuring from the center of the 45 cm cube downward. The turbine is designed for operation at an optimal wind speed of 11 meters per second, with a predicted tip speed ratio of 2.25 and is able to maintain a constant angular velocity and power output when experiencing wind speeds from 11 to 22 meters per second. Note that the tip speed ratio refers to the ratio between the wind speed and the speed of the tips of the blades and can be found using the equation $\lambda = \frac{\omega R}{V_\infty}$, where λ is tip speed ratio, ω is the turbine's rotational speed, R is the turbine's radius, and V_∞ is the freestream wind velocity. The turbine also needs to have the ability to adapt to changing wind direction through a yaw control system. The system must also be able to withstand wind speeds up to 25 meters per second when parked and also have an emergency shutdown sequence that can greatly slow or stop the rotor both with a manual switch or when separated from the PCC.

In order to meet the design requirements stated above, certain components and systems were needed. It is desired that the turbine blades are able to maximize available wind capturing volume while remaining strong and lightweight. For this reason, they were designed with a 3D printed skeletal structure reinforced with a carbon fiber skin. Pitch control for a cycloturbine can be performed in a variety of ways, which are shown in **Figure 2**. One such method is an active control design, where the pitch of the blade is controlled by a linear actuator. Active control requires a complex electrical control system to constantly change the pitch throughout the turbine rotation. Instead of a complicated electrical control system, a passive mechanical control scheme has been used. The passive mechanical control system implemented in this design uses a mechanical cam and roller mechanism for simplicity, while integrating a robust factor into the design. A traditional fixed pitch VAWT performance is not dependent on wind direction. However, a variable pitch cycloturbine performance relies heavily on the directionally dependent pitching scheme. As such, it was necessary to develop an active control yaw system within the design to properly orient the pitching scheme. The optimum pitch is directly related to the tip speed ratio. The power coefficient (C_p) of the system can be described as the ratio of the power generated by the turbine and the total power available from the wind. Some pitching schemes have an easier time self-starting and ramping but have a lower maximum power coefficient, while others will make the cycloturbine unable to start from standstill but can achieve a much greater power coefficient once they are up to speed. For this reason, multiple stages of pitching schemes are implemented in the design.

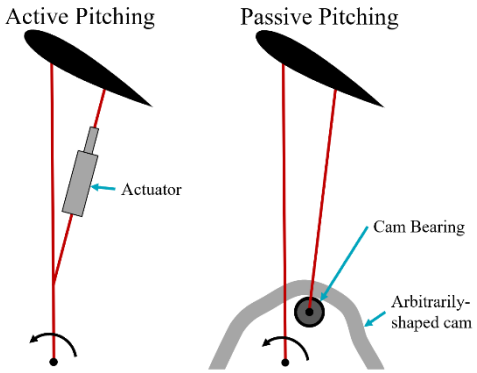

Figure 2: *Blade pitching methods*

Power development is achieved with a permanent magnet synchronous generator which was chosen for its relative simplicity and high efficiency. A planetary gearbox was implemented to convert the optimum operation speed of the rotor assembly into the optimum operational speed of the generator so that maximum performance and efficiency can be achieved.

All of these subsystems and components need to work together in a compact design that ensures structural stability, minimal friction and energy loss, and operational reliability. This mechanical design is discussed further in **Section IV**. The system is controlled by an Arduino based microcontroller which monitors a variety of variables such as wind speed, rotor speed, and output voltage which is discussed

further in **Section V**. In order to properly design these systems for maximum performance, an accurate understanding of the underlying aerodynamics is required.

III. Aerodynamic Design

A. Aerodynamic Analysis

While cycloturbines perform better than fixed pitch VAWTs do, they are more difficult to analyze. Some wind turbine aerodynamic software packages, such as QBlade, have the capability to analyze VAWTs, but those analyses are less accurate than those for HAWTs, and they do not have the capability to analyze cycloturbines. To analyze our cycloturbine, we developed our own blade-element momentum codes to implement flux-line theory, a low-order model developed specifically for cycloturbines. Flux-line theory is a new method for analyzing cycloturbines developed by Zach Adams and Jun Chen, two researchers at Purdue who first published about it in 2017 [1]. Our flux-line theory codes were implemented in MATLAB and were written jointly by a member of the aerodynamics team and the team advisor, Dr. Taub. We contacted Adams and Chen, who helped us understand some of the theory.

Flux-line theory is a type of momentum model. **Figure 3** shows how flux-line theory differs from previous momentum models. Momentum models use actuator disk theory, which is a simplified model of complex blade-fluid interactions used for rapid calculations of an unknown flow-field. An actuator disk is an infinitely thin disk where momentum is instantaneously removed from a streamtube. Actuator disks model momentum transfer from a fluid to a blade at low computational cost. HAWTs can be easily modeled with this theory using a single streamtube and actuator disk, as seen in **Figure 3A**. Since the turbine spins

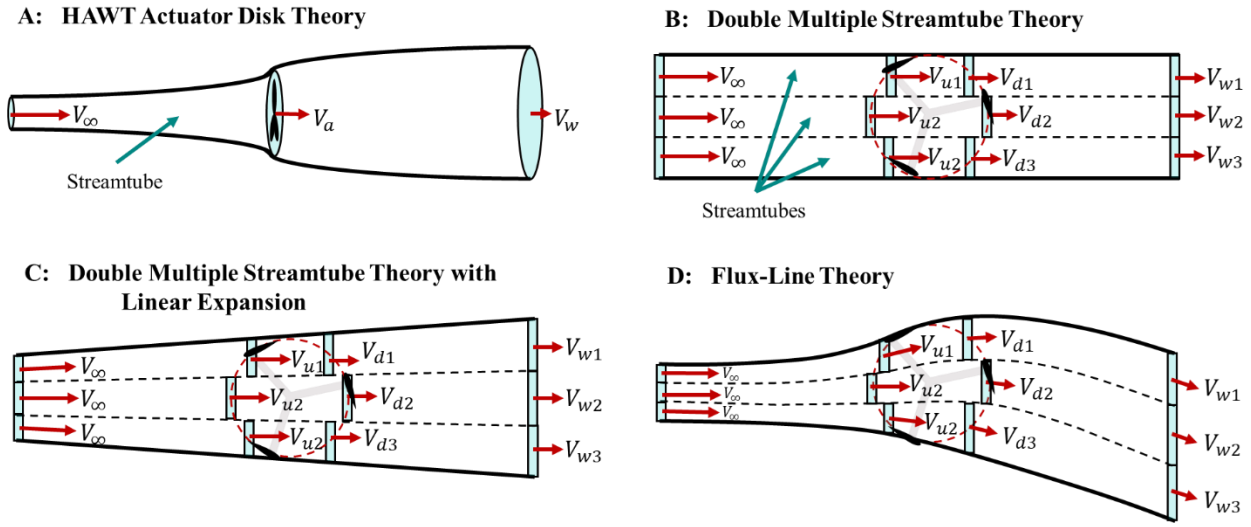

Figure 3: *Progression of streamtube models*

in a plane, only one actuator disk is needed. The entire turbine interacts with the streamtube at only one location. However, this is not true for VAWTs, which require more complicated streamtube models.

For a VAWT, all air passes through the turbine twice, once on the upstream side of the turbine and once on the downstream side. This means that to accurately model the turbine, each streamtube needs two actuator disks. Additionally, unlike HAWT blades, the way VAWT blades interact with the air around them is dependent upon their angular position within the turbine's rotation. VAWT blades can produce lift on one side of the turbine and be completely stalled on the other side. This means that air passing through the

turbine does not undergo uniform deceleration. Because of this, VAWT streamtube models need to be discretized into many streamtubes.

One way to do this is to use a double multiple streamtube model, which is what QBlade uses for its fixed-pitch VAWT analysis [2]. These models are relatively simple to compute, but, as **Figure 3B** shows, they use streamtubes of constant cross-section. They are not able to model flow expansion as it is decelerated, as the HAWT actuator disk theory does. A modification to this model allows flow expansion, but assumes it is linear. Double multiple streamtube models with linear expansion (**Figure 3B)** assume that flow expands uniformly as it passes through the turbine, which is a simplification the model needs to make to work but is not true. The rate of flow expansion is dependent on the velocity change within each streamtube, which is not constant for a VAWT. Flux-line theory is a new streamtube model which allows streamtubes to both bend and expand [1], as shown in **Figure 3D**. It makes fewer assumptions about the shape of the streamtubes than previous models do and has been shown to predict more accurate results.

Figure 4 shows the flux-line theory streamtube model. Each streamtube is analyzed at four points, or *flux-lines*, which is where the theory gets its name. Each streamtube has its properties calculated in the freestream flow, at the upstream and downstream flux-lines (which trace the paths of the blades), and at the wake flux-line. At the upstream and downstream flux-lines, the angle γ dictates how much the streamtube bends. The length of the flux-lines are not fixed, which allows for flow expansion. The downstream flux-line can be longer than the upstream one, as the flow decelerates and expands.

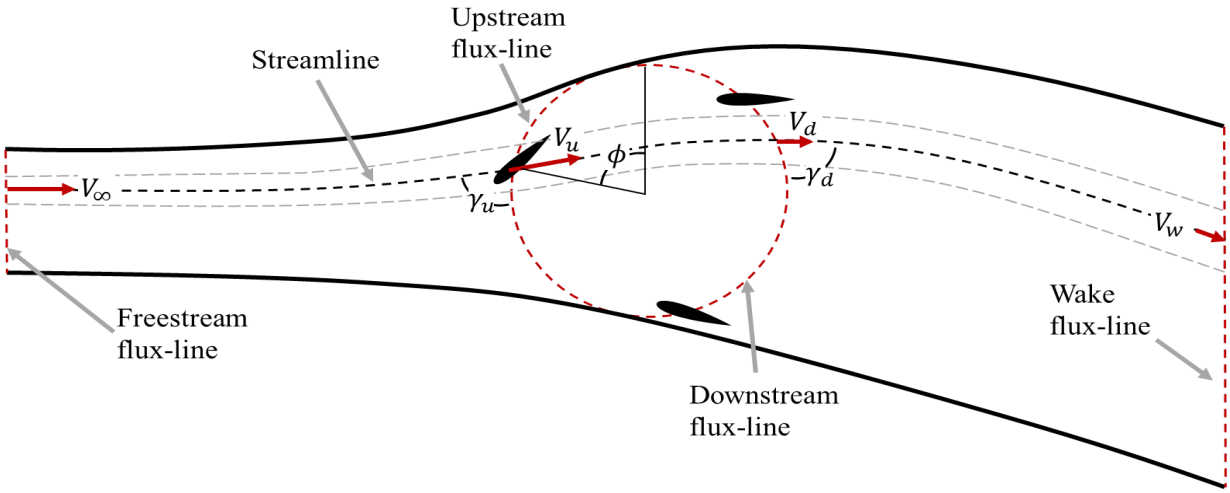

Figure 4: *Flux-line theory*

Flux-line theory has two variations: a blade-element model and pure momentum theory. The blade-element model is an iterative method used for performance prediction. It uses blade-element momentum theory. It takes inputs such as the airfoil profile, pitching scheme, tip-speed-ratio to calculate how much momentum is imparted to the turbine blades based on a guessed wind velocity. It uses this information to balance the momentum within each streamtube and reevaluate the streamtube velocities at each flux-line. It then repeats this process until it converges upon a solution where momentum transferred to the blades matches the momentum taken from the streamtube. When convergence is reached, the turbine power is calculated from the forces that the model has determined are applied to the blades.

The blade-element model is useful for the performance prediction of a cycloturbine if the blade pitching scheme is known, but it is computationally expensive, and would be cumbersome to use to optimize a pitching schedule. For this, the pure momentum model is more helpful. The pure momentum model calculates turbine power from the velocity distributions along each flux-line and determines which velocity distribution would produce the highest power coefficient. It is essentially the reverse of the blade-

element model. Instead of calculating velocity distributions for a given pitching function, it optimizes a velocity distribution, then determines what pitching function would produce that distribution.

To design our turbine pitching scheme, we used pure momentum theory to take optimal velocity distributions as predicted by Adams and Chen [3], and predict what blade pitching scheme would be necessary to slow the air down in that way. Pure momentum theory is a somewhat simplified version of the blade-element model. It only considers blade lift; one of its assumptions is that blade drag is negligible. Pure momentum theory has formulas for relating blade lift coefficients to velocity distributions, from that, we calculated what lift coefficient would be required at each position around the turbine to get the velocity distribution suggested by Adams and Chen, and from that we could calculate what blade angle would have that lift coefficient. However, to know the relationship between blade angle and lift, we required an airfoil polar. Airfoil polars are readily available for airfoils in a straight flow, but VAWT blades experience a curved flow, called *curvilinear flow*. This is shown in **Figure 5**.

Figure 5 shows one of the effects of curvilinear flow, which is that a blade does not experience a uniform angle of attack (α), as blade in a straight (or *rectilinear*) flow would. Commonly available airfoil polars are only valid in rectilinear flow. There are two things that cause these polars to be invalid, one is that airfoils in curvilinear flow have varying local angles of attack along the chord length, and the second thing is that the boundary layer of air around airfoils is susceptible to centrifugal forces, called *centrifugal loading*. Conformal mapping techniques can be used to account for the variation in angle of attack, but very little research has been done on the effect of centrifugal loading. Additionally, the effects of centrifugal loading vary with rotational speed, so VAWT airfoil polars are dependent upon their tip-speed-ratio. Direct experimental data for a given airfoil and turbine geometry is required to get curvilinear airfoil polars. We had planned to conduct experiments on airfoils to determine their polars, but this was not possible due to COVID-19. In their paper, Adams and Chen [2] give their experimentally determined airfoil polars, and although those are for a different airfoil than we had, we used their polars in all our codes. They used a NACA 0012, and we picked a NACA 0018. Both airfoils are symmetrical, which is common for VAWTs, because airfoils need to produce either positive or negative lift depending on where they are, but NACA 0018s seemed to work better on some simple small-scale models we had made previously. Also, NACA 0018s are thicker than NACA 0012s and more likely to endure the CWC's high wind speeds. Again, we had planned to test airfoils ourselves, but this was not possible.

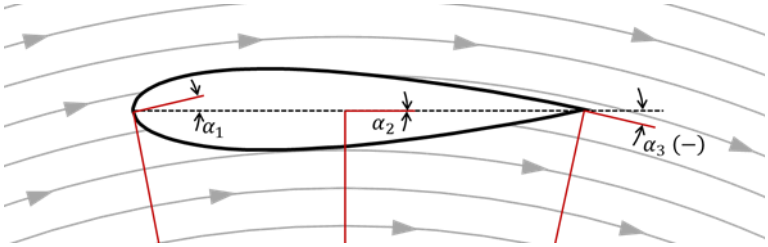

Figure 5: *Curvilinear flow*

Using Adams' and Chen's method for translating optimal velocity distributions to blade pitching motions, we obtained the optimal pitching schedules for tip speed ratios of 0.5 and 2.25. An example of this is shown in **Figure 6**.

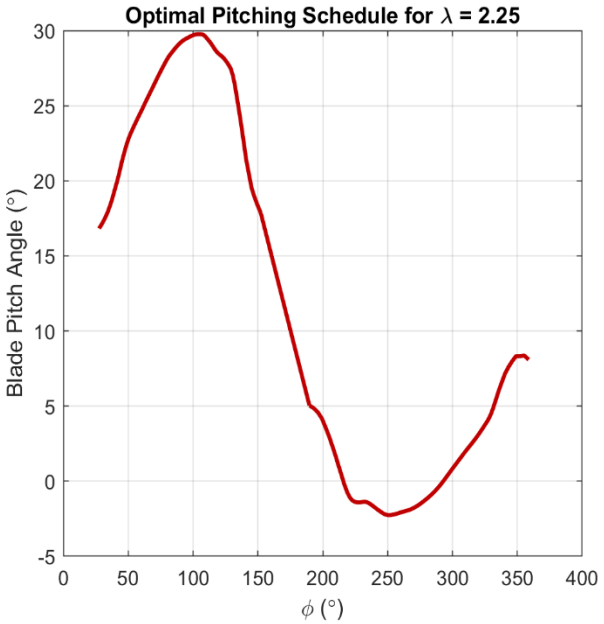

Figure 6: *Optimal pitching schedule as determined by our pure momentum theory code. ϕ represents the angular position of a turbine blade, as shown in* ***Figure 4****.*

The details of this process can be found in our code, which is available upon request, and in Adams' and Chen's paper [3]. The pitching schedules shown are what we determined would slow the air down to the optimal distributions given by Adams and Chen. The information in **Figure 6** shows good agreement from the data in the paper by Adams and Chen [3], and we believe our pure-momentum code is working correctly.

B. C_P-λ Curve

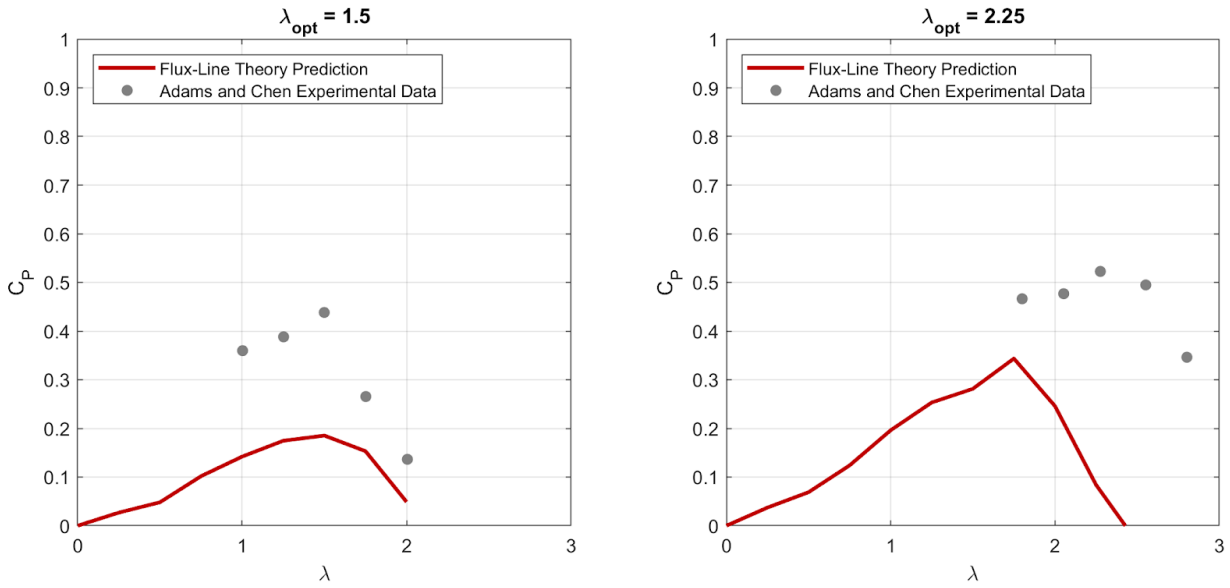

Figure 7: *C_P-λ curve as predicted by our blade-element code, compared to Adam's and Chen's experimental data for a turbine with geometry scaled off ours.*

The geometry of our turbine was scaled off the geometry of Adams' and Chen's turbine for two reasons: so that we could use their airfoil polars, and so we could validate our results with theirs. Adams and Chen built a cycloturbine and reported their experimental data. We used this data to evaluate the predictions of our blade-element code. Our C_P-λ curve was generated with the blade-element version of flux-line theory. It can be seen in **Figure 7**. The figure has two plots, the one on the right is the prediction for our turbine with a cam optimized for a tip speed ratio of 2.25. The plot on the left is for additional comparison between the predictions of our model and experimental data. **Figure 7** shows that our blade-element model is currently underpredicting power coefficients. Our code is nearly operational, but still in the debugging stage, as its development was delayed by COVID-19. We suspect that the experimental data collected by Adams and Chen more closely represents the C_P-λ curve that our turbine would have, but we would like to verify this with experimental data. Our plans for this are detailed more in **Section VI**. Our actual

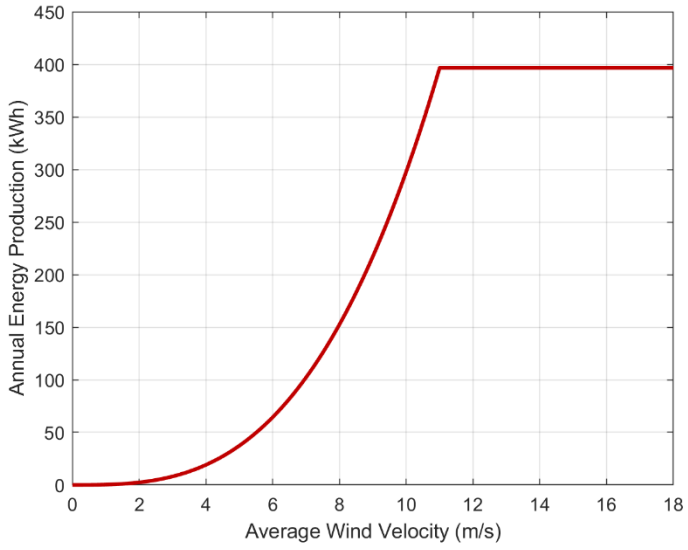

Figure 8: *Annual Energy Production*

C_P-λ curve would likely be lower than the one gathered by Adams and Chen, but we think it would be roughly in the same place. While our turbine geometry was scaled off theirs, they had a much larger turbine than we did. Because our design is so much smaller than theirs, our turbine is much more vulnerable to frictional losses, which would likely lower our power coefficient.

The annual energy production of our turbine can be seen in **Figure 8**. The figure is based on three assumptions: that the power coefficient is about 0.35, (the highest predicted by our blade-element model), that the turbine produces constant power above wind speeds of 11 m/s, and that the density of air is 0.96 $\frac{kg}{m^3}$, which is it's value in Denver, Colorado, the intended location for the CWC testing.

IV. Mechanical Design

A. Design Overview

Our cycloturbine design can be seen in **Figure 9**. The vertical axis wind turbine design employs three composite airfoils that are equally spaced, with their centerlines each 120 degrees apart. A precision stainless steel rod is used for the main shaft and consists of a ¾ inch lower shaft and a ½ inch upper shaft. The upper shaft is concentrically fitted to the lower shaft through a tight tolerance slip fit and fastened with a bolt. The lower shaft sits in two cylindrical roller bearings which are integrated into the fixed turbine housing. Two bearings are used to create a support couple for the rotor assembly, resisting any moments induced by rotational imbalance and vibration. A shoulder on the lower shaft locates the shaft vertically

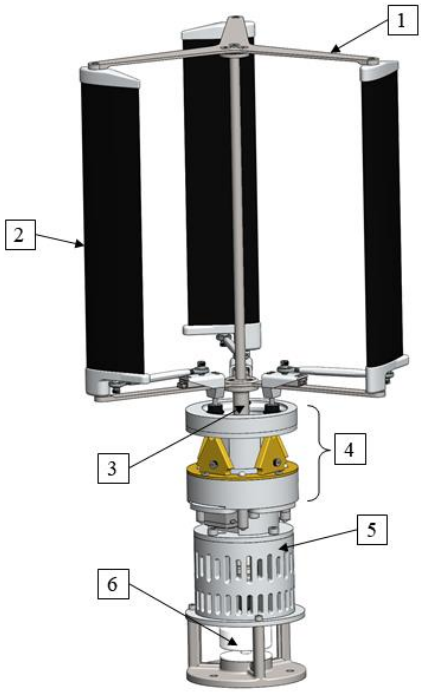

Figure 9: *The complete turbine assembly. The assembly includes the rotor arms (1), airfoils (2), main shaft (3), cam and lifter assembly (4), main housing (5), and anemometer (6)*

and rests on the inner race of the upper bearing. The bottom of the lower shaft is threaded for a low-profile nylon locking nut which is used to keep the shaft from lifting during rotation. **Figure 10** shows the configuration of the main shaft assembly.

The nylon locking nut serves a dual purpose, as it can be tightened in order to add preload to the bearings. Preload is needed to properly seat the rollers into the bearing races and reduce wear within the bearing. The main shaft extends down into the housing through the braking system and engages the planetary gearbox. Stainless steel upper and lower rotor arms are fastened to flanges on the top and bottom of the exposed main shaft. These hold the rotor assembly together, provide the pivot points for the airfoils, and support the variable pitch components. The airfoil pivot points incorporate bearings to help minimize friction as the airfoils are pitched at various angles throughout rotation.

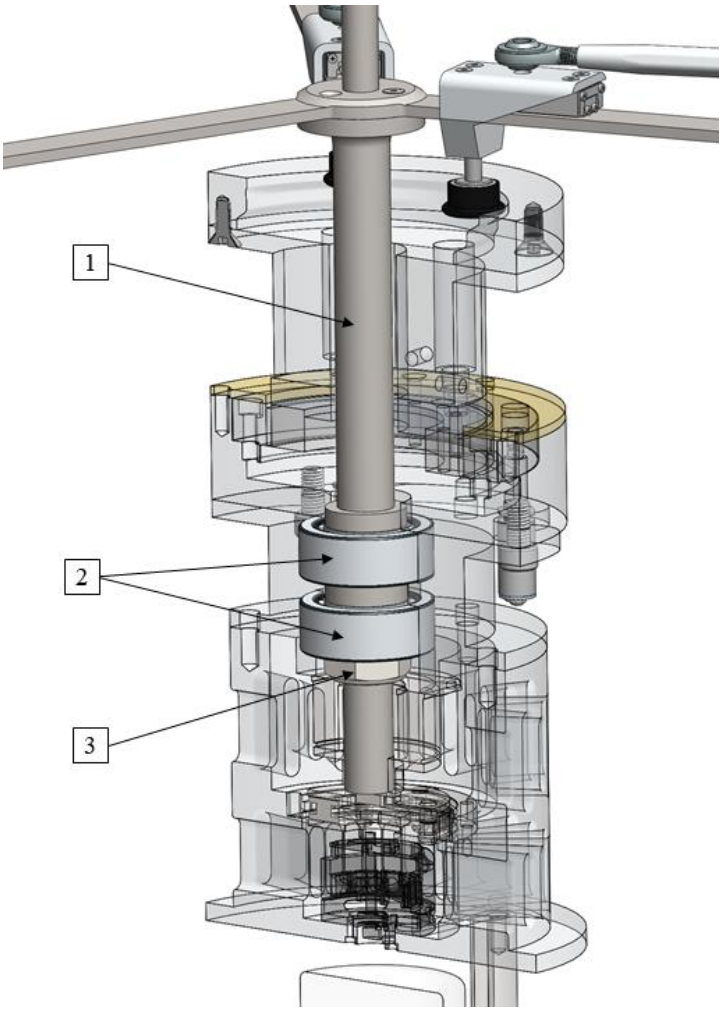

Figure 10: *Main shaft assembly. Rotor arms are attached to the exposed main shaft. Lower Main Shaft (1) Main Shaft Bearings (2) Shaft Lock Nut (3)*

In order to achieve continuously changing airfoil pitch throughout the entirety of the rotation, a cam mechanism is used, which is shown in **Figure 11**. An internal cam consists of a modified circular profile that has an infinitely changing distance from the center axis of rotation. An ideal cam profile is determined for a particular tip speed ratio, as previously discussed in **Section III**, and is incorporated as the cam ring interior surface. Cam roller bearings attached to the rotor hold contact with this interior surface. The follower bearings translate this motion into linear motion through low friction linear slide bearings. The linear motion is then transmitted to the airfoils by linkage arms which pivot the airfoils about the rotor arm mounts. Each airfoil is independently controlled by the cam interior profile. This operation controls each airfoil and continuously provides pitch control throughout the system rotation. The use of this interior cam system provides complete control of the pitch and can be tested and tuned to maximize turbine performance. In order to ensure consistent contact between the cam and the rollers, a torsion spring housing is built into the lower airfoil cap. This spring induces a constant moment on the airfoil which pushes the cams up against the interior cam surface. Once the rotor is up to operating speed, the radial acceleration of the system will be the predominant factor in maintaining this contact.

Unlike a VAWT with a fixed blade pitch, a cycloturbine can vary its blade pitch in order to optimize the performance of the turbine. The optimal blade pitch depends on the wind velocity and current. The cycloturbine needs a yaw system to account for changing wind direction. The turbine is capable of correcting for changes in wind direction through the yaw control of the cam, which is shown in **Figure 12**. Rather than rotating the airfoils towards the wind like with a HAWT, our system makes windage adjustments through the yaw control of the pitch scheme cam. The cam platform is fastened to a rotating roller ring bearing that allows for a full 360 degrees of rotation. Mounted into the housing below the cam platform is a continuous rotation servo. The servo uses a 16-tooth gear to engage a larger 84 tooth gear

which is attached to the rotating portion of the base. This arrangement allows the servo to make yaw adjustments to the cam based on wind direction input signals. The angular position is continuously being checked and corrected throughout turbine operation. In the lower section of the turbine, mounted in the

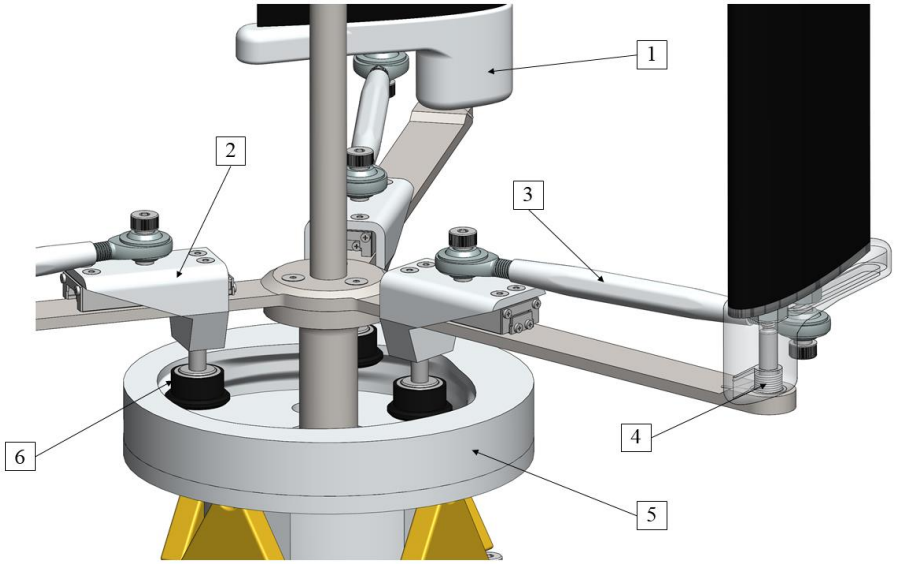

Figure 11: *Rotor Cap (1) Linear Slide bearing System (2) Pitch Control Linkage (3) Torsion Spring (4) Cam (5) Cam Roller Bearing (6)*

very center of the housing column is an ultrasonic anemometer. Due to the size constraints and the nature of the turbine design, a mechanical wind vane control was not ideal. Instead, a non-mechanical wind measuring device was implemented and an ultrasonic anemometer was chosen. This sensor is capable of four readings per second, sensing wind speed and direction with a full 360-degree scope. The sensor being mounted in the center of the lower section ensures consistent readings of less turbulent flow regardless of the direction of incoming wind. The stainless-steel housing for the anemometer is designed to minimize airflow interference while maintaining structural integrity to support the rest of the turbine assembly during operation.

The optimal pitch scheme is a function of the systems tip speed ratio. To have an efficient turbine, the system must be able to adapt to different tip speed ratios and adjust pitching schemes accordingly. This has been addressed by developing a multiple stage cam system that enables the pitching scheme to change. The current design allows for three profile transitions. The top profile is a startup and low speed pitching scheme and is set to be optimal at a TSR of 0.5. The middle profile is a high-speed profile that optimizes performance at a TSR of 2.25. The lowest and final profile is a curbing profile designed to reduce the lift generated by the airfoils in order to maintain control of the system at extreme wind speeds. During operation, the turbine sensors are continuously checking the tip speed ratio and when a specified threshold is reached, a sequence of operations takes

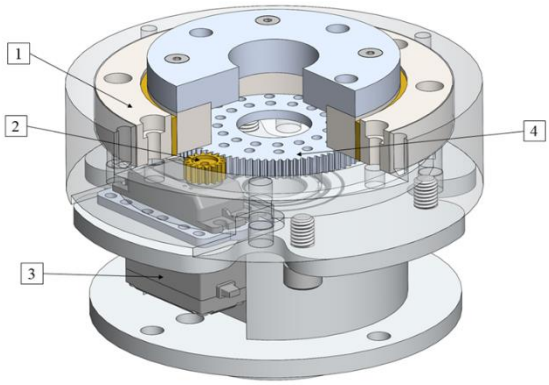

Figure 12: *Yaw adjustment system. Parts include the roller ring bearing (1), a 16-tooth gear (2), a continuous rotation servo (3), and an 84-tooth gear (4).*

place to change the pitching scheme. This change is achieved through raising and lowering the cam, thus changing the contact surface between the cam and the cam roller bearings. During regular operation and yaw adjustment, there are four evenly spaced low friction bronze triangular lifters that slide about a similarly low friction sliding surface. These triangular lifters are mounted to the cam platform using high precision shoulder bolts, shown in **Figure 13** and **Figure 14**. The shoulder bolts maintain a set distance and path for the lifters to slide about and also allow for them to rotate. The lifters are able to transition from sliding on one of the triangular faces to another. The lifters are also mounted on the shoulder bolts such that the distance between the lifter sides and center of rotation is different for each side by an increment of 0.25

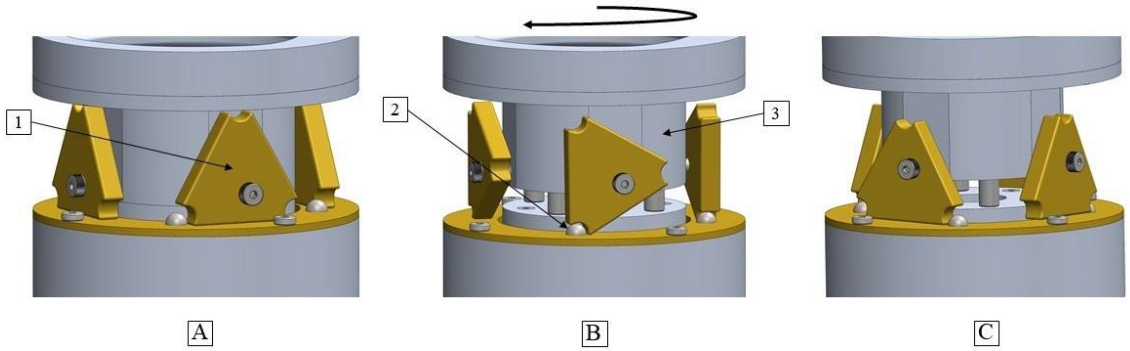

Figure 13: *Multiple stage cam system, which is enabled through the use of lifters (1). The lifters are tripped through the raising of actuator pins (2), which in turn lifts the cam platform (3) into one of three distinct profiles.*

inches. Mounted into the housing beneath the lifters are four equally spaced linear actuators. When a profile transition takes place, these actuators are powered on and lift actuator pins up into position for engagement with the lifters. The yaw control servo is then temporarily repurposed to be the driving force in lifting up the cam. This is done by swiftly rotating the cam assembly 90 degrees. As the lifters slide this distance, their corners simultaneously engage with the actuator pins. This creates a force couple resulting in a 60-degree rotation of the lifter, transitioning the lifter from one sliding surface to the next. The result is the cam being lifted or lowered as needed, depending on the direction of the sequence. Four large precision shoulder bolts are used as guide pins to allow the cam platforms change in height and compression springs are used to maintain secure contact between the lifters and the sliding surface.

One design objective is to have the ability to maintain a constant power output and angular velocity during operation with varying wind conditions. This is achieved through the implementation of an electromagnetic friction brake, as shown in (annotation 1 in **Figure 15**), that is fastened to the turbine main shaft within the housing before the gearbox. The electromagnetic brake consists of a base which holds the electromagnet and one of the two friction plates. The other friction plate is attached by a spring plate to a flange mounted to the turbine shaft. The spring plate applies constant force, pulling the friction plate away from the magnet. The base is mounted stationary with respect to the turbine shaft while the flange is spinning. To apply the brake, an electric current is supplied to the magnet pulling the two friction plates together and induces a torque to the shaft, in the opposing direction of motion. This brake has the ability to maintain a desired rotor velocity and resulting power output.

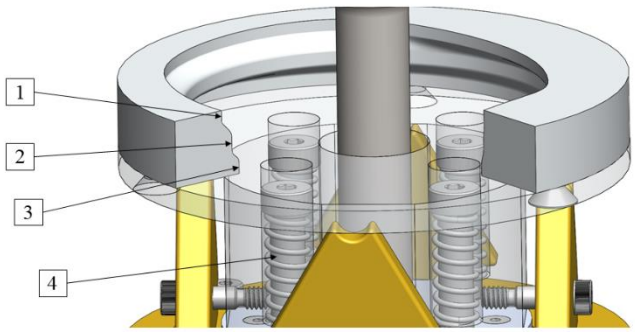

Figure 14: *Section view of the 3D cam and it's three interior profiles. The three profiles are the start-up and low-speed profile (1) with a tip speed ratio 0.5, the operational high-speed profile (2) with a tip speed ratio of 2.25, and the lift reduction*

The turbine can implement a safety shutdown procedure and drastically reduce angular velocity even in high speed wind

conditions. Two systems are used to ensure the rotor assembly can safely and quickly come to a halt. The third profile of the variable pitch control cam is a curbing profile which is designed to greatly reduce the lift generated by the airfoils. When this third pitching scheme is engaged, the drag forces on the system will overpower the lift forces being generated. In addition to this, the control brake can be fully engaged. These two factors combined will cause the turbine to stop operation. The cam can then be lowered back down to the low speed pitching scheme and the brake can be fully disengaged to allow the rotors to be fully operational once again.

The generator being used in the turbine has a greater, more efficient power output when operating at speeds much higher that the turbine is able to produce alone. Because of this, a gearbox is installed into the housing which engages the main shaft between the braking system and the generator, which is shown in **Figure 15**. This is a planetary gearbox that increases the shaft angular velocity by 5 times while maintaining concentricity.

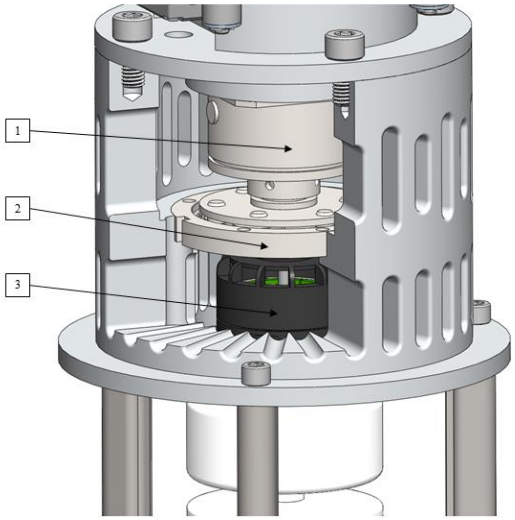

Figure 15: *Section view for the system containing the electromagnetic friction brake (1), the planetary gearbox (2), and generator (3)*

B. Mechanical Loads

The rotor will experience mechanical loads due to vibration, centrifugal, and wind forces; the most prominent being centrifugal loads due to the continuous rotation of the turbine. In comparison to the centrifugal and vibrational forces experienced by the turbine, the wind load is minimal and is therefore ignored for the following analysis. The mechanical sources of load include the springs and rollers used in the pitching scheme as described in Section IV. SolidWorks was deemed insufficient to accurately calculate these loads as they will vary with friction and mechanical alignment. These loads will be analyzed once a physical prototype is built and is available for testing.

Vibrational forces on the system depend on the mass symmetry and balance of the rotor. Static and dynamic techniques can be used to balance the rotating assembly. All rotor components of the assembly will be weighed to ensure mass similarity. A static balance will be done to determine the location of any imbalanced weight once the rotor assembly is complete. The goal is to have the weight of all components distributed equally about the center of rotation. A dynamic balance test can also be performed while the turbine is in rotation using a dynamic balance measuring device. It is important to note that although the device may be balanced with fixed airfoil pitch, the assembly will be inherently imbalanced due to the dynamic pitching scheme.

To test the strength of the rotor, centrifugal loads were applied in the finite element studies. Using the designated tip speed ratio of 2.25 as the operating condition yielded a maximum rotational velocity of 1074 RPM, rounded to 1100 RPM for simpler calculations. The maximum rotational velocity was calculated for use in finite element analysis (FEA) and a minimum factor of safety (FOS) of 2 was chosen to ensure the rotors do not yield. Using a similar method for a maximum wind velocity of 25 meters per second and maximum tip speed ratio of 2.5, a rotational speed of 2700 RPM was deemed to be the maximum runaway speed in the event of a braking failure. It would be unlikely that the turbine would reach this rotational speed, but these values were tested in order to ensure that failure would not occur in any worst-case scenario.

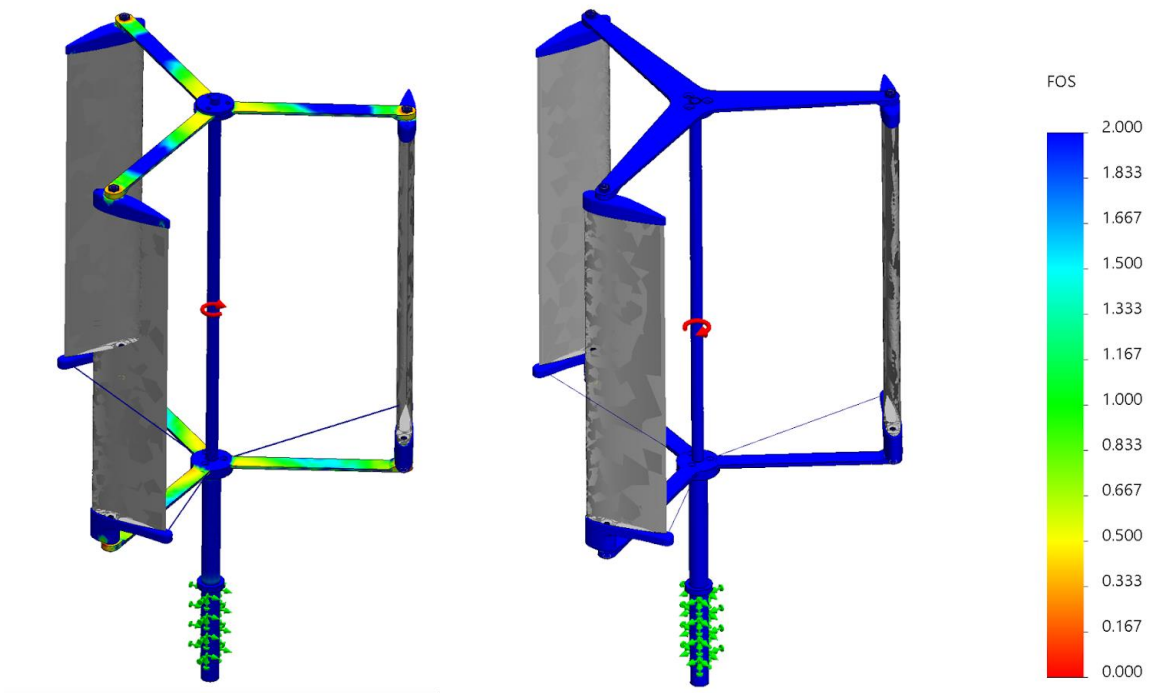

Figure 17: *Side by side comparison of initial rotor arm design (left) and final rotor arm design (right). Both studies are completed at the maximum design rotation of 1100 RPM (112.5 rad/s)*

The airfoils are to be built with a carbon fiber shell and a skeletal interior structure which cannot be analyzed accurately using SolidWorks simulation features, as the system is missing information on the deformation properties. For the sake of analysis, these airfoils were modeled as a rigid body. The expected actual masses from the first prototype were used to override the mass calculated in-program. This FEA was done to analyze the rotor arms, airfoil caps, and main shaft of the rotor assembly. During the Rotor Strength Test milestone, the airfoils showed no yielding or damage when the rotor was tested to failure at 1000 RPM. As these were not the weak points of the design, they were therefore not considered a critical component in our strength analysis.

Many of the assembly components such as the cam roller mechanism and tie rods come with manufacturer recommended maximum loads. In the FEA, these components have been modeled as rigid links and motion analysis can be used to determine if these maximum capacities will be reached.

As seen in **Figure 17**, the initial rotor arm design did not reach the desired FOS for the maximum expected rotational speed. After the first analysis, slight adjustments were made to the upper and lower arms. The lower thickness was increased from 0.125 inches to 0.157 inches. The upper arms were strengthened with a large fillet and taper. Both the upper and lower arms were originally 6061 aluminum but were modified to be 304

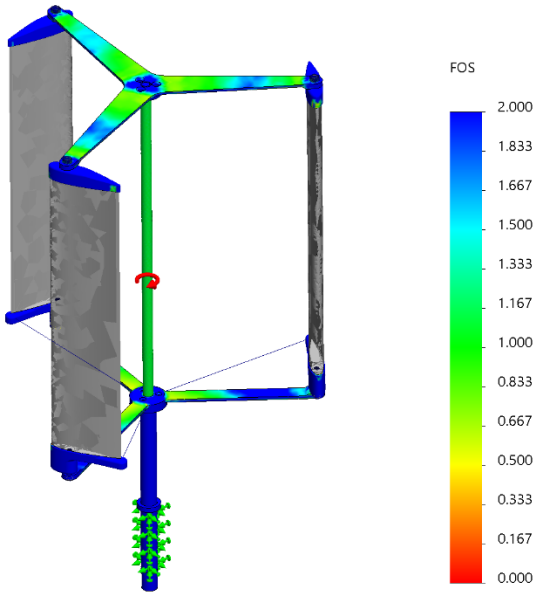

Figure 16: *Final rotor arm design at 2700 RPM, the theoretical maximum RPM if the braking system failed*

stainless steel. The results of this alteration can be seen in **Figure 17**, where the entire tested design achieves the goal FOS of 2.

This redesigned rotor was then analyzed at the expected catastrophic failure speed as shown in **Figure 16**. As we do not expect the rotor to reach this rotational speed, this study was done to see which parts of the rotor arms are likely to yield at the current design. The majority of the rotor is above a FOS of 1, and so we expect these regions of the rotor to survive the catastrophic rotational speed. The areas below the FOS of 1 will likely experience strain hardening but are unlikely to experience fracture. We will verify all FEA results through physical testing after the turbine has been built as there are several factors not accounted for, including the aforementioned wind and mechanical loads, that are most easily and accurately found through direct testing.

V. Electrical Design and Controls

A. Electrical Analysis

The goal of this design is to reliably convert the mechanical energy of the rotor to a constant DC voltage source. The design is based around a permanent magnet synchronous generator (PMSG), the Multistar Elite 3510. Asynchronous and DC generators were avoided due to added complexity of the system and lower efficiencies respectively. With an optimal rotational speed of approximately 5000 RPM, and 14 poles, we expect an electrical input frequency of 3.7 kHz. The power electronics of the generator are controlled by an Arduino Uno microcontroller.

We are using a passive 3-phase rectifier (**Figure 18**). In order to accommodate fast switching speed and allow high efficiency with passive components, our rectifier will use Schottky diodes. After the rectification stage we use a buck-boost converter to generate a constant 12V DC output voltage, and a secondary buck converter to generate 5V DC power for the microcontroller and sensors. The DC-DC converters are controlled from PWM signals coming from the main Arduino unit, which monitors both converters' output voltage.

Comparators are used to monitor the safety features, monitoring output current and the state of the kill switch. When the load is disconnected from the turbine, the output of the comparator will trigger an interrupt on the main controller unit. The controller will then initiate shutdown procedures, safely slowing the turbine to the specified low speed.

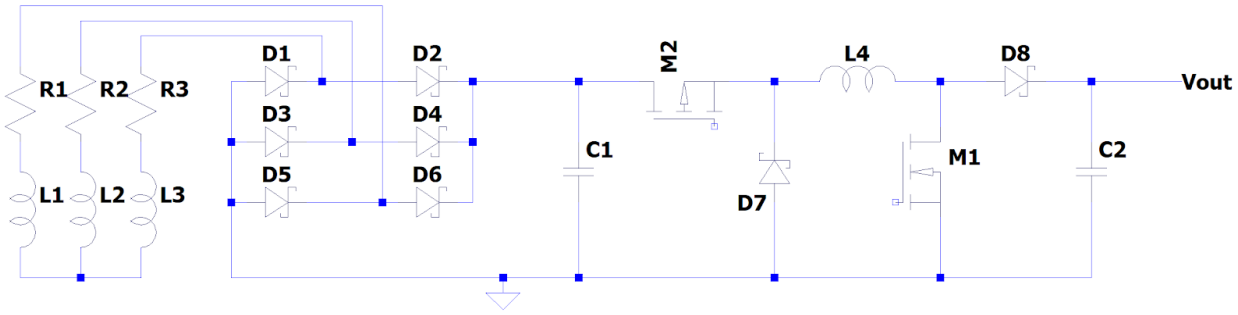

Figure 18: *Generator and power electronics model*

B. Control System

The goal of the turbine's control system in normal conditions (e.g. load connected, no emergency stop signal) is to maximize power production while maintaining safe operating conditions. To achieve this

a variety of sensors and actuators (listed in **Table 1**) are combined with an Arduino microcontroller to form a control loop. In the event that an emergency stop is necessary the cam, yaw, and friction brake can all be used to slow the rotor to an acceptable speed.

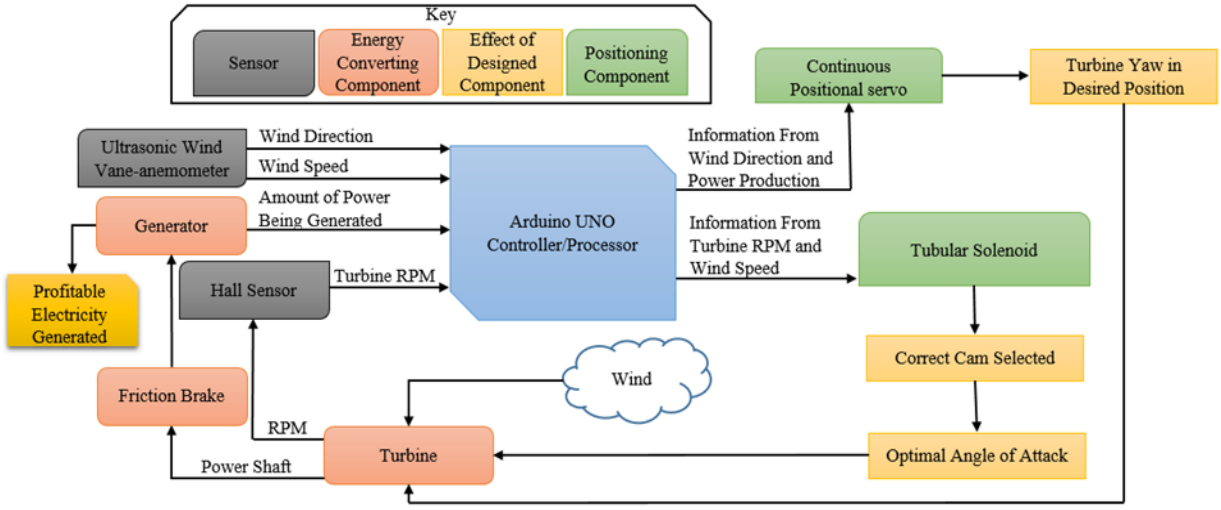

Figure 19: *Generator control block diagram*

A constant rotor speed between 11 meters per second and 23 meters per second must be maintained. An ultrasonic anemometer and Hall effect sensor are used to monitor wind and rotor speeds respectively, data from which is fed into the microcontroller. Based on this data adjustments are made to the yaw of the turbine, pitch of the blades, and activate the friction brake when necessary. The anemometer has a secondary purpose of measuring wind direction, which in conjunction with a rotary encoder monitoring yaw angle is used to control a positional servo. This causes the cam to rotate to match the direction of the wind which in turn optimizes power production.

Information on the generator's power production is provided by monitoring a phase current I_A and a line to line voltage V_{AB}. The power production in combination with the tip speed ratio (TSR), as determined by rotor and wind speeds, is used to determine if adjusting the stage of the cam is needed. For measured TSR less than unity the cam level designed for a TSR of 0.5 will be used, and when the measured TSR exceeds unity the cam level designed for a TSR of 2.5 will be used.

Data logging and user input is accomplished through Excel Data Streamer. An interface was created using Arduino to send/receive data to/from Excel. Digital filters and PID controllers' objects were defined in Arduino C in order to allow for flexible changes to control loops. When we build the turbine, these will be used to construct a control loop as seen in **Figure 19**.

Table 1: *List of sensors and actuators used in the control system*

Sensor	Model	Actuator	Model
Hall Effect Sensor	US5881LUA	Friction Brake	Miki Pulley 112-05-11
Ultrasonic Anemometer	CV7-E-OEM	Solenoid for Cam Lifters	GEEPLUS 130-H
Rotary Encoder		Positional Servo	
Ammeter	ACS712		

VI. Experimental Verification

To test our prototype turbines, a wind tunnel with a large industrial fan was constructed. The wind tunnel was built around a CWC spec turbine and can be seen in **Figure 20**. The tunnel is intended to also serve as a safety enclosure for runaway testing. For this reason, it features a heavy-duty wood construction to withstand impacts from any projectiles and contain damage in the event of structural failure. **Figure 20** shows a student measuring the wind velocity profile in the test section with a hot-wire anemometer. The wind tunnel has a draw-down configuration, in which the fan sucks air through the test section. Inside the test section, the wind tunnel reaches a speed of approximately 7 m/s.

Figure 20: *Wind tunnel constructed for runaway test*

Figure 21: *First prototype*

Earlier in the year, we were able to construct one prototype which we used for our runaway test. This prototype is shown in **Figure 21**. Our first prototype used a simple sinusoidal cam design, not a flux-line optimal one. We tested this turbine in our wind tunnel to determine its C_P-λ curve, but for this particular model, the curve was very low. The C_P-λ curve was determined by using a driven dynamometer which could vary the braking torque applied to the turbine shaft, and measure both this torque and the turbine's rotational speed. It would have been ideal to continue this testing with future prototypes, but this was not possible due to school closures. The first prototype had some mechanical issues that were addressed in later designs, we would like to test our new designs in the wind tunnel to see how much they have improved.

We look forward to using our wind tunnel to experimentally determine curvilinear airfoil polars, as was discussed in **Section III**. Curvilinear airfoil polars are needed for our flux-line theory code to make accurate predictions, and we could have gotten them if we had access to our labs. Curvilinear polars need to be found by spinning airfoils and measuring the forces on them, they cannot be measured by conducting tests on just an airfoil, which is how rectilinear polars are found. We had planned to use our prototype to set airfoils at known angles, then use a dynamometer to spin the prototype turbine at different speeds to measure the drag on the airfoils, which we

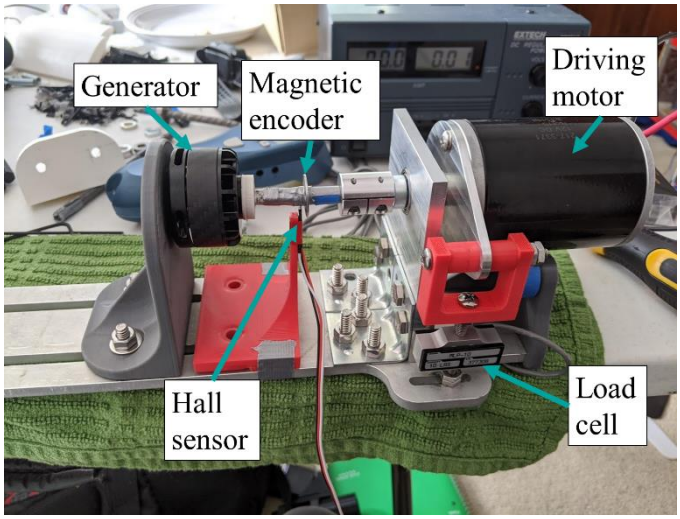

Figure 22: *Driving dynamometer coupled to generator*

could then relate to lift. These tests would be conducted inside the wind tunnel as a safety measure, to keep parts from flying off. The tests would be conducted while the wind tunnel was turned off. Running the tests in the zero-wind condition makes it easy to know the angle of attack the blades are experiencing, as it would be constant for all the blades. The cyclically varying angles of attack a cycloturbine sees in normal operation would be gone, making the data much easier to analyze. We would like to conduct this test when we regain access to our labs.

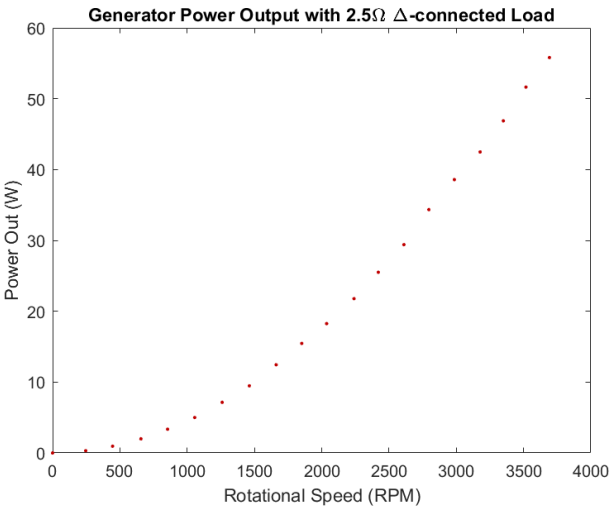

Figure 23: *Measured generator power output*

We also built a driving dynamometer to test our electrical design with. **Figure 22** shows the dynamometer coupled to the generator we chose for our prototype. The dynamometer is constructed from a motor mounted on bearings supported by a load cell. The load cell prevents the motor from rotating and allows us to measure the amount of torque on the generator. The rotational speed of the dynamometer is measured with a Hall-effect sensor and a magnetic encoder. The driving motor of the dynamometer was chosen to mimic the rotor and is capable of producing low speeds. We intended to use the dynamometer with a gearbox to get power curves for our motor, but we did not have a gearbox picked out before school closures and could not get one during the resulting quarantine.

During the quarantine, we continued dynamometer testing at home to get power curves for our generator. **Figure 23** shows the extent of the generator power curve we were able to collect without a gearbox to increase the speed of the shaft driving the generator. A lack of electrical components prevented us from further testing, but we would like to continue this work when we have access to our labs again. We plan to test our power electronics by applying a variety of constant torques with the dynamometer and using an oscilloscope to measure the mean value and frequency spectrum of the system's output voltage as per the power quality measurement milestone. We will then use this data to determine if additional filtering is needed and make necessary changes to the DC-DC converter's control loop. We plan on investigating methods to deliver initial power to the control system such as bootstrapping and initially drawing power from the load.

VII. Conclusion

The Washington State University Everett Wind Energy team, in collaboration with Everett Community College Wind Energy team, designed a cycloturbine for CWC 2020. The team has spent the year strengthening our understanding of wind energy concepts and applying such an understanding to our project development. Although the collaborative effort made by the two schools cannot be put to use in competition this year, the design will be tested and improved in the year to come. Cycloturbine aerodynamics are an area of active research, and we would like to contribute to that with our prototype. Additionally, much of this year was spent developing our own blade-element momentum codes to implement flux-line theory for cycloturbines. These codes have reached a stage which requires experimental data to move forward in these developments. The data needed can be collected with this new prototype once it has been built and will help verify our code and make further improvements to the blade elements. The team built and tested the first iteration of the cycloturbine with promising results. We were able to learn from this process and greatly improve the design in the second iteration.

The prototype will also be used as a test bench for next year's designs. A functional physical prototype will assist in modification and improvement of various system elements such as pitching scheme combinations and airfoil geometries. A physical prototype will also help the improvement of our electrical design. Observing the system response will allow us to make changes to the electrical design and explore a variety of methods to accomplish each task. We will also be working on active rectification of generator power to allow for increased efficiency and electrical speed control. Continued research and design will make way for more powerful and efficient iterations for years to come. As soon as the team has access to school facilities and manufacturing resources, we plan on beginning the manufacturing process. The many unique components of the assembly require precise manufacturing processes in order to achieve tight tolerances and desired results. The planning and creation of a novel idea such as the implementation of a 3D internal cam system brings with it a host of challenges. Similarly, the development of new applications for flux-line theory is a laborious task. Exploring new avenues has been the driving force in motivating the team and overcoming these challenges. The true end goals for the team are to gain experience and a greater understanding of wind energy concepts and the engineering process. This year has laid the groundwork for future years of competition in which the team can continue to work towards these goals.

References

[1] Z. Adams and J. Chen, "Flux-Line Theory: A Novel Analytical Model for Cycloturbines," *AIAA*, vol. 55, no. 11, pp. 3851-3867, 11 2017.

[2] D. Marten and J. Wendler, "QBlade Guidelines," 2013.

[3] Z. Adams and J. Chen, "Optimization and Validation of Cycloturbine Blade-Pitching Kinematics via Flux-Line Theory," *AIAA*, vol. 56, no. 5, pp. 1894-1909, 2018.